Resource

Cell Reports

Modeling Cerebrovascular Pathophysiology in Amyloid-β Metabolism using Neural-Crest-Derived Smooth Muscle Cells

Graphical Abstract

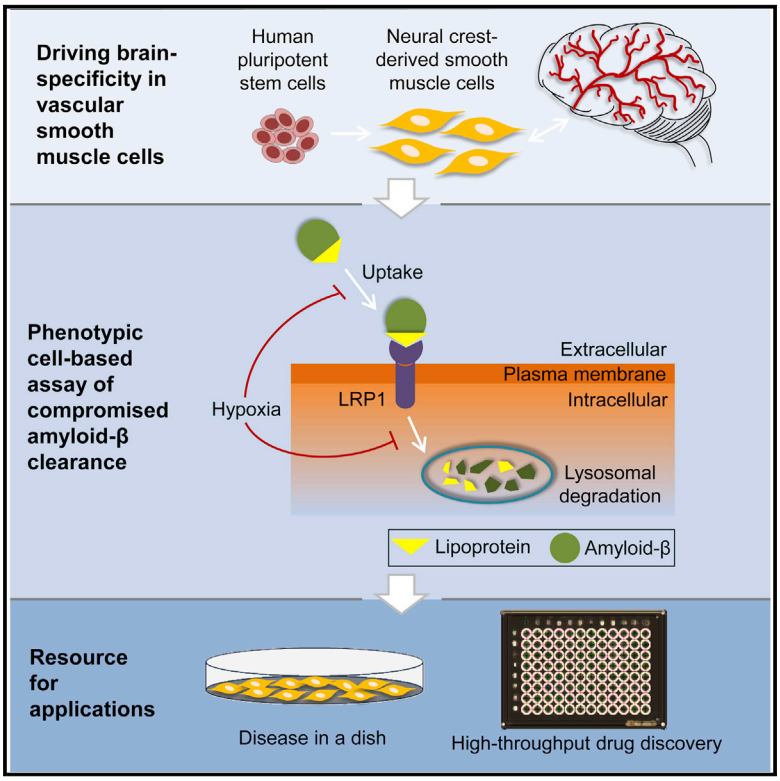

Highlights

Neural crest-derived vascular SMCs to model cerebrovascular SMCs

Differential amyloid-β uptake by SMC subtypes of different embryonic origins

Cell-based assay of amyloid-β uptake for high-throughput phenotypic screening

Authors

Christine Cheung, Yeek Teck Goh, ..., Chenghan Wu, Ernesto Guccione

Correspondence

ccheung@imcb.a-star.edu.sg

In Brief

The contribution of blood vessel pathologies to neurodegenerative disorders is relatively neglected, partly due to inadequate human tissues for research. By using human stem cells, Cheung et al. establish a method of generating vascular smooth muscle cells (SMCs) from neural crest progenitors, the primary precursors that give rise to brain blood vessels. These stem-cell-derived SMCs display defective amyloid processing under chronic hypoxia, a phenomenon well documented in the cerebral vasculatures of aged people and patients with Alzheimer's disease.

Accession Numbers

GSE55173

Cheung et al., 2014, Cell Reports 9, 391–401
October 9, 2014 ©2014 The Authors
http://dx.doi.org/10.1016/j.celrep.2014.08.065

Cell Reports
Resource

Modeling Cerebrovascular Pathophysiology in Amyloid-β Metabolism using Neural-Crest-Derived Smooth Muscle Cells

Christine Cheung,[1,2,*] Yeek Teck Goh,[1] Jingxian Zhang,[1] Chenghan Wu,[3] and Ernesto Guccione[1,4]
[1]Institute of Molecular and Cell Biology, 61 Biopolis Drive, Proteos, Singapore 138673, Singapore
[2]Department of Medicine, Yong Loo Lin School of Medicine, National University of Singapore, 1E Kent Ridge Road, NUHS Tower Block, Singapore 119228, Singapore
[3]Faculty of Medicine, Nursing and Health Sciences, Monash University, 246 Clayton Road, VIC 3168, Australia
[4]Department of Biochemistry, Yong Loo Lin School of Medicine, National University of Singapore, Singapore 119074, Singapore
*Correspondence: ccheung@imcb.a-star.edu.sg
http://dx.doi.org/10.1016/j.celrep.2014.08.065

SUMMARY

There is growing recognition of cerebrovascular contributions to neurodegenerative diseases. In the walls of cerebral arteries, amyloid-beta (Aβ) accumulation is evident in a majority of aged people and patients with cerebral amyloid angiopathy. Here, we leverage human pluripotent stem cells to generate vascular smooth muscle cells (SMCs) from neural crest progenitors, recapitulating brain-vasculature-specific attributes of Aβ metabolism. We confirm that the lipoprotein receptor, LRP1, functions in our neural-crest-derived SMCs to mediate Aβ uptake and intracellular lysosomal degradation. Hypoxia significantly compromises the contribution of SMCs to Aβ clearance by suppressing LRP1 expression. This enabled us to develop an assay of Aβ uptake by using the neural crest-derived SMCs with hypoxia as a stress paradigm. We then tested several vascular protective compounds in a high-throughput format, demonstrating the value of stem-cell-based phenotypic screening for novel therapeutics and drug repurposing, aimed at alleviating amyloid burden.

INTRODUCTION

Neurodegenerative disorders such as Alzheimer's disease affect millions of people globally and pose major public health challenges. Amyloid plaques and neurofibrillary tangles are the primary hallmarks of Alzheimer's disease. There is now an increasing recognition that the vascular system could play a causative role to some of these pathologies in the brain. Amyloid-beta (Aβ), a peptide processed from the amyloid precursor protein (APP), drains from the brain with interstitial fluid and becomes deposited in the blood vessels walls as cerebral amyloid angiopathy (CAA) (Soffer, 2006). CAA is implicated in 80% of Alzheimer's disease patients and 10%–40% of elderly without Alzheimer's disease (Jellinger, 2010; Viswanathan and Greenberg, 2011). Down's syndrome patients also have prominent CAA because of duplication of the APP locus, resulting in elevated Aβ burden (Rovelet-Lecrux et al., 2006; Sleegers et al., 2006). In normal physiology, cellular uptake and subsequent proteasomal degradation of Aβ are the principal means of metabolizing Aβ with little accumulation in the central nervous system (Nedergaard, 2013). Extracellular elimination routes also play a part in clearance through the blood-brain barrier and transportation to liver. Cerebrovascular smooth muscle cells (SMCs) and astrocytes are known to be able to remove Aβ locally via the low-density lipoprotein receptor-related protein 1 (LRP1)-mediated endocytic pathway (Kanekiyo et al., 2012). On the other hand, LRP1 reductions have been reported in Alzheimer's disease patients and LRP1 also appears to decrease significantly with age (Deane and Zlokovic, 2007). Brains of patients with severe CAA are often exposed to chronic hypoxia due to cerebral blood dysregulation and microhaemorrhages (Farkas and Luiten, 2001). Previous studies have demonstrated that hypoxia is associated with lowered LRP1 expression in cerebral SMCs (Bell et al., 2009). LRP1 downregulation in vascular cells may lead to dysfunctional local Aβ processing, exacerbating the growth of para-arterial Aβ deposits in CAA. Secondary neuronal degeneration may further cause cognitive impairment and dementia. Therefore, the need to identify therapeutic interventions targeting neurovascular complexities is critical.

Animal models have been indispensable for the studies of CAA (Winkler et al., 2001; Herzig et al., 2004). Considering the caveat of interspecies disparity, judicious interpretation is required when extrapolating results from animal research to human biology. Drug discovery has traditionally relied on immortalized target-expressing cell line and human primary cells for screening. The limitation of the former is the lack of biological interactome whereas the latter often has too much batch-to-batch variation, and is difficult to obtain in sufficient quantities. It would be valuable to develop a human in vitro system that simulates the pathophysiological characteristics of cerebral vasculatures. The advent of human pluripotent stem cells (hPSCs) such as embryonic stem cells (hESCs) and induced pluripotent stem cells (iPSCs) could provide a source of SMCs for modeling pathological processes in CAA to facilitate interrogation of molecular mechanisms.

There is compelling evidence that SMCs in different regions of the vasculature originate from diverse embryonic lineages

(Majesky, 2007). In CAA, Aβ accumulation occurs predominantly in the wall of intracerebral and leptomeningeal arteries (Soffer, 2006), both of which are derivatives of the neural crest lineage (Li et al., 2013). Here, we report the generation of SMCs from hPSCs via a neural crest population. We found that SMCs of various embryonic origins had different extent of compromised Aβ uptake upon hypoxic treatment and that LRP1 regulated Aβ processing in our neural crest-derived SMCs. Finally, we developed a phenotypic assay of Aβ uptake and validated it by pilot screening of pharmaceutical compounds in a high-throughput format.

RESULTS

Derivation of Neural Crest-Specific Vascular SMCs

The majority of studies to date have focused on the generation of generic SMCs, which may confound potential lineage-specific differences (Cheung and Sinha, 2011). We and others have attempted the derivation of origin-specific SMCs from hPSCs (Cheung et al., 2012; Wang et al., 2012). For the purpose of modeling cerebral SMCs, we tested different chemical cocktails based on factors known to promote neural crest differentiation in hPSCs (Chambers et al., 2009; Menendez et al., 2013) (Figure S1A). Because activation of canonical Wnt signaling had shown to induce neural crest formation in hPSCs, we tested an inhibitor of glycogen synthase kinase 3, CHIR99021. Bone morphogenetic protein (BMP) antagonist noggin was included to counteract mesodermal induction due to endogenous BMP signaling in hPSCs. A combination of basic fibroblast growth factor (bFGF, 12 ng/ml), activin/nodal inhibitor SB431542 (10 μM), noggin (200 ng/ml) resulted in peaked expressions of neural crest markers between days 10 and 16 of hPSC (hESC H9) differentiation (Figure 1A). We monitored the development of neural crest surface markers (Figure S1B) and found that both FSb (bFGF + SB431542) and FSbN (bFGF + SB431542 + noggin) conditions yielded substantial amount (>65%) of double NGFR and B3GAT1 expressing cells on day 10. Isolated $NGFR^+/B3GAT1^+$ cells from FSbN treatment confirmed greater expression levels of neural crest genes than those from FSb treatment (Figure 1B). Hence, these $NGFR^+/B3GAT1^+$ cells were purified, following FSbN treatment, to perform subsequent differentiation into vascular SMCs.

We adopted our previous SMC differentiation protocol (Cheung et al., 2012) to differentiate this intermediate neural crest population using platelet-derived growth factor BB (PDGF-BB, 10 ng/ml) and transforming growth factor-beta 1 (TGF-β1, 2 ng/ml) for another 12 days. The resultant neural crest-derived SMCs (NCSMCs) were then characterized in comparison to neuroectoderm-derived SMCs (NESMCs) (Cheung et al., 2012) and positive control, human brain vascular SMCs (BVSMCs). The source of BVSMCs used in this work has been employed in several studies as a model of human cerebrovascular SMCs (Kanekiyo et al., 2012; Lefterov et al., 2010; Zuloaga and Gonzales, 2011; Yao et al., 2014; Shi et al., 2014). A panel of SMC-related genes was upregulated in all SMC subtypes derived from both hESCs (H9) and iPSCs (BJ-iPSCs) as compared to hPSCs (Figure 1C). NCSMCs demonstrated comparable levels of TAGLN (Figure 1D), an actin crosslinking protein found in smooth muscle, and contractile protein ACTA2 (Figure 1E), as NESMCs and BVSMCs. Furthermore, NCSMCs exhibited contractile ability with reduction of cell surface area in response to a vasoconstrictor, angiotensin II (Figure 1F). Waves of calcium influx were detected by fluo-4 imaging during contraction (Figure S1C; Movies S1, S2, S3, and S4). These results verified that the NCSMCs were functional. To determine whether our $NGFR^+/B3GAT1^+$ neural crest population was indeed multipotent, we carried out neuronal differentiation (Hu and Zhang, 2009). The neural crest cells were found to give rise to network structures stained positive for neuronal markers TUBB3 and MAP2 (Figure S1D).

NCSMCs Demonstrate Cerebrovascular-Relevant Amyloid-β Uptake Ability

To model after cerebrovascular SMCs with high fidelity, we investigated whether NCSMCs shared the closest molecular signatures and functional characteristics with BVSMCs than the SMC subtypes originating from other embryonic origins (e.g., neuroectoderm, lateral plate mesoderm, and paraxial mesoderm) (Cheung et al., 2012). Unless otherwise stated, most experiments were performed using SMC subtypes were derived hESC (H9). Gene expression analysis showed that NCSMCs derived from either hESCs (H9) or iPSCs (BJ-iPSCs) clustered more closely with BVSMCs than NESMCs in the gene ontology (GO) category of brain development (Figure 2A; genes listed in Table S1). Functional annotation of the commonly enriched genes in all SMC subtypes indicated GO categories such as blood vessel development and extracellular matrix organization as expected (Figure S2A). Common genes specific only to BVSMCs and NESMCs demonstrated functions pertaining to blood vessel development, but there were also irrelevant GO categories like skeletal system and bone development. On the other hand, NCSMCs seemed to share more specialized functions with BVSMCs in integrin-mediated pathway (adhesion), epithelial cell differentiation (necessary for neural crest specialization), response to calcium (contractile ability), and smooth muscle development. Hence, we postulated that BVSMCs could resemble more closely to NCSMCs than NESMCs.

Because oxygen deprivation could be an initiating event in the pathogenesis of CAA, we cultured the various SMC subtypes at 1% oxygen for at least 2 weeks to induce chronic hypoxia. All the SMC subtypes responded with an upregulation of hypoxia-inducible factor-1α (Figure S2B). Internalization of Aβ by lipoprotein receptors on SMCs was reported to be compromised by hypoxic conditions (Bell et al., 2009). Low-density lipoprotein receptor (LDLR) mediated Aβ uptake and cell death of cerebral perivascular cells (Wilhelmus et al., 2007). Cerebrovascular cells and neurons also express different Aβ-degrading enzymes including neprilysin (MME), tissue plasminogen activator (PLAT), and matrix metalloproteinases (Zlokovic, 2011). MME is downregulated in both hypoxia (Wang et al., 2011) and Alzheimer's disease patients manifesting CAA (Miners et al., 2006). By gene expression quantification, we found that *LRP1*, *LDLR*, *MME*, and *PLAT* were significantly downregulated in a majority of the SMC subtypes, with the greatest reduction observed in NCSMCs and NESMCs compared to their counterparts that were cultured at 21% oxygen (Figure 2B). Protein

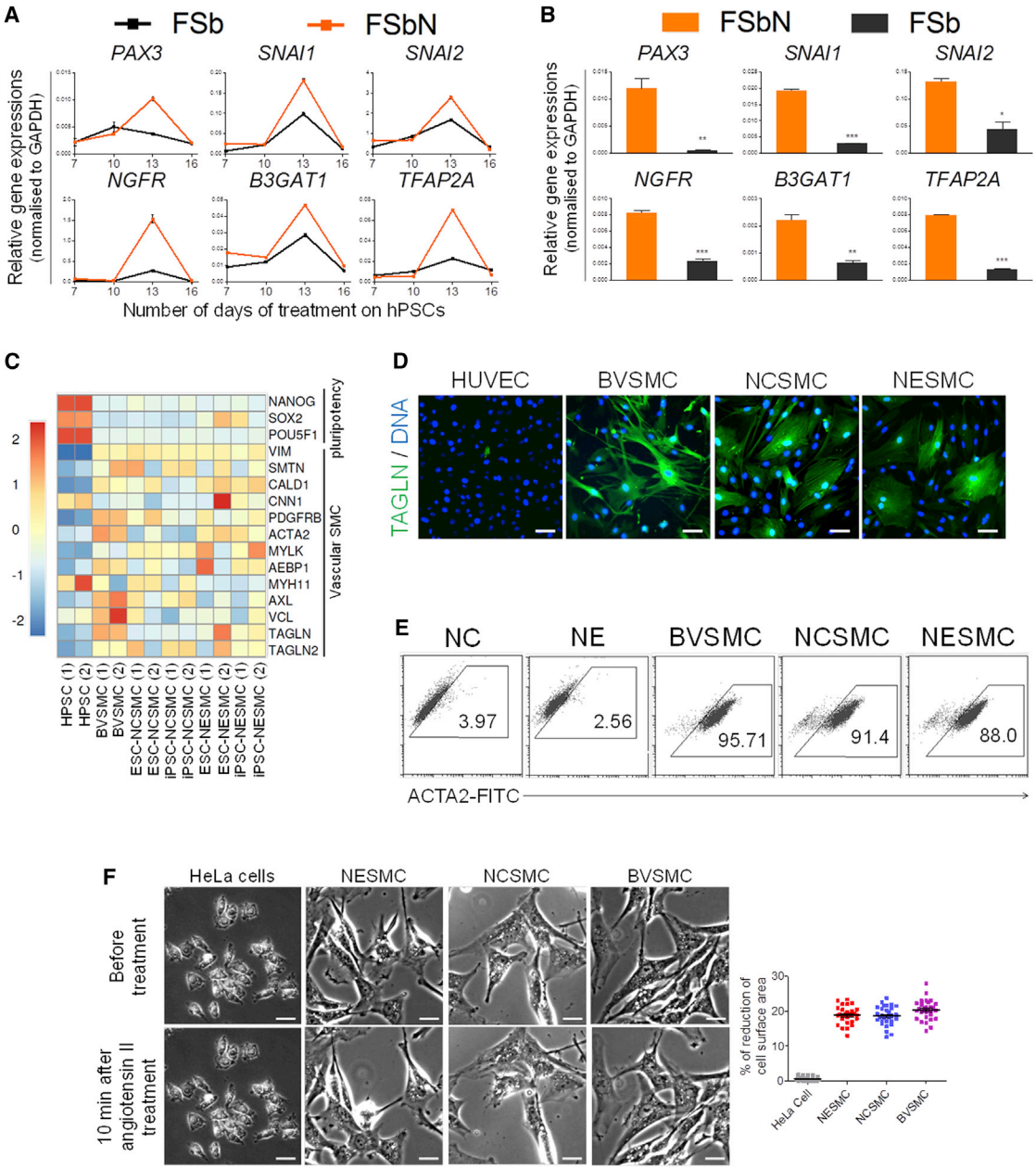

Figure 1. Characterizations of Neural Crest-Derived Vascular SMC

(A) Quantitative RT-PCR of neural crest markers during FSb (bFGF + SB431542) and FSbN (bFGF + SB431542 + noggin) treatments on hPSCs. FSbN was more effective than FSb at inducing neural crest gene expressions between day 10 and day 16.

(B) FACS-sorted NGFR$^+$/B3GAT1$^+$ cells from FSb- and FSbN-treated populations were profiled for neural crest genes. Data represent means ± SEM (n = 3). Statistical differences compared to FSbN samples were calculated with Student's t test (*p < 0.05, **p < 0.01, **p < 0.001).

(C) Microarray gene expression heatmap of SMC markers in hPSCs versus positive control, human brain vascular SMCs (BVSMCs), neural crest SMCs (NCSMCs), and neuroectoderm SMCs (NESMCs) obtained from hESC (H9) and iPSCs (BJ-iPSCs) after differentiation. Orange (upregulation) and blue (down-regulation) depict differential gene expression from the mean across all samples.

(D) NCSMCs, NESMCs, and positive control, BVSMCs, were immunostained positively for SMC contractile protein, TAGLN. Human umbilical vein endothelial cells (HUVECs) were used as a negative control.

(E) Flow cytometric analysis of SMC protein, ACTA2, in NC and NE before SMC differentiation, as well as in NCSMCs and NESMCs after differentiation. Numbers on the plots indicate percentage of ACTA2$^+$ cells. A substantial proportion of cells in each SMC subtype was positive for ACTA2 (88%–95%).

(F) All SMC subtypes displayed contractile ability in response to angiotensin II. HeLa cells were used as a negative control. There was 18%–21% reduction of cell surface area in contracting SMCs. Data represent means ± SEM (n = 30). Scale bar, 50 μm.

See also Figure S1.

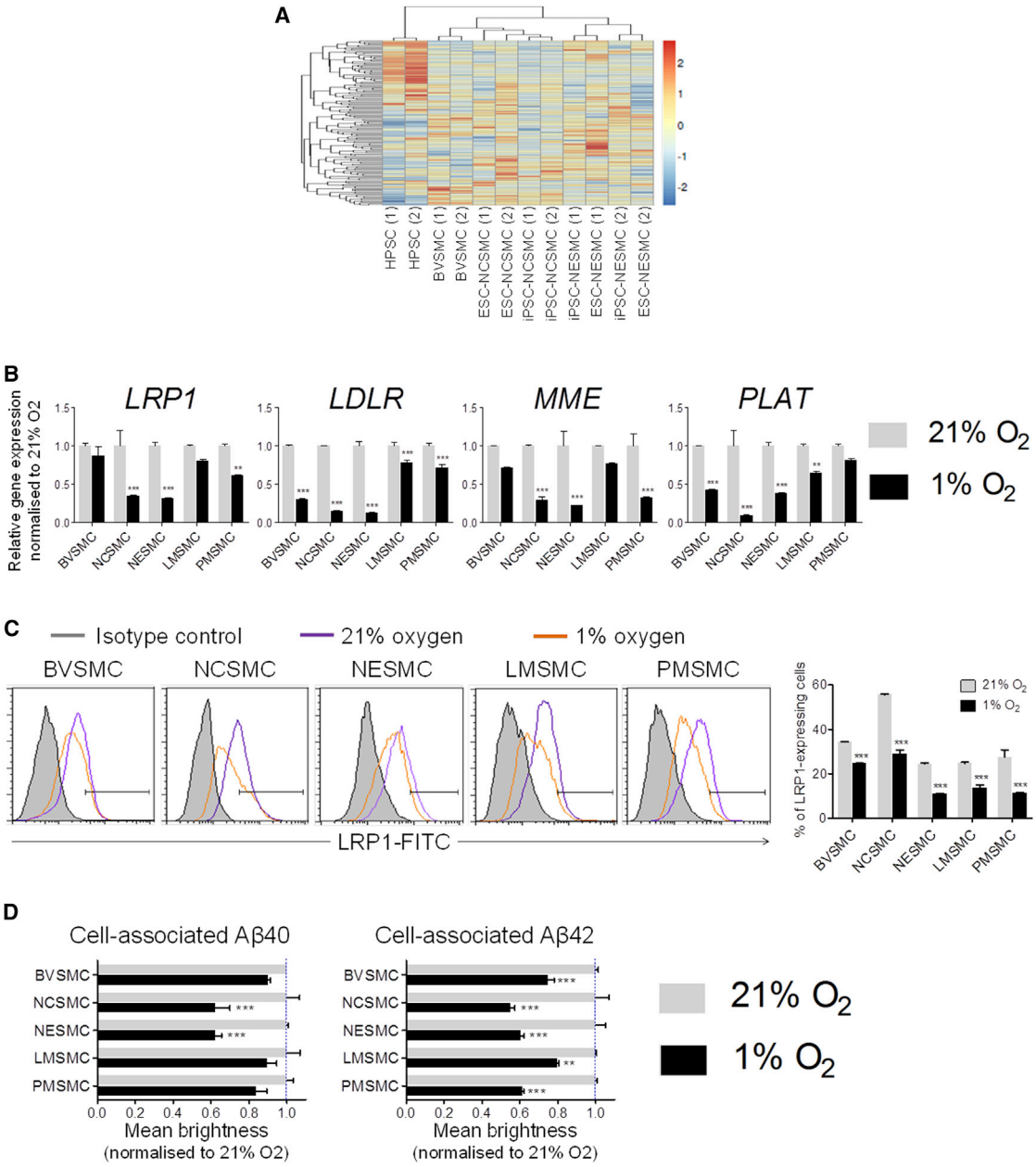

Figure 2. Chronic Hypoxia Compromises Aβ Uptake Differentially in SMC Subtypes

(A) Clustering of genes from the gene ontology category of brain development revealed that the molecular signatures of NCSMCs associated more closely with BVSMCs than NESMCs.

(B) A comparison of the effect of 21% versus 1% oxygen on the gene expressions of lipoprotein receptors and Aβ-degrading enzymes in different SMC subtypes.

(C) Flow cytometric analysis of the percentage of $LRP1^+$ cells in SMC subtypes. One percent oxygen significantly decreased LRP1 expression in all SMC subtypes. The black bars on the histogram plots demarcate the gating for quantifying the percentages of LRP1-expressing cells.

(D) Uptake of fluorescently labeled Aβ40 and Aβ42 peptides by SMC subtypes after 3 hr was measured by flow cytometry. Cell-associated Aβ was calculated as mean brightness of the cells with Aβ uptake as a ratio to their respective no-uptake control cells at 21% and 1% oxygen.

Data represent means ± SEM (n = 3). Statistical differences compared to 21% oxygen samples were calculated with ANOVA (*$p < 0.05$, **$p < 0.01$, ***$p < 0.001$). Statistical differences compared to day 0 were calculated with ANOVA (†$p < 0.001$). See also Figure S2.

analysis showed decreased percentage of LRP1-expressing cells in the SMC subtypes at 1% oxygen (Figure 2C). LRP1 is abundantly expressed in the cerebral vasculatures, in particular, the SMCs (Lillis et al., 2008). We found that more than 50% of NCSMCs expressed LRP1, constituting to the highest percentage of $LRP1^+$ cells among the SMC subtypes (Figure 2C, right panel). Taking into consideration the difference in abundance of LRP1 protein per cell, the median fluorescent intensity of

LRP1-FITC in each of the SMC populations also decreased significantly at 1% oxygen (Figure S2C).

Aβ40 is the chief form of vascular amyloid component in CAA, whereas Aβ42 may be responsible for early-stage damage (Alonzo et al., 1998). Aβ deposits in parenchyma and blood vessels seem to be originated from neuronal-derived Aβ as animal studies indicated that local production of Aβ by cerebrovascular cells was not essential to drive CAA pathology (Winkler et al., 2001; Calhoun et al., 1999). To examine hPSC-derived SMCs' ability to uptake exogenous Aβ, we first treated BVSMCs with fluorescently labeled Aβ40 and Aβ42 peptides (2 μg/ml). Aβ internalization via LRP1 requires the presence of serum lipoprotein (Urmoneit et al., 1997). At different time points after the onset of Aβ uptake in serum-containing media, we measured the mean fluorescence brightness by flow cytometry to determine the amount of cell-associated Aβ in BVSMCs (Figure S2D). The rate of Aβ uptake slowed down after 3 hr, so we carried out 3 hr Aβ uptake for subsequent experiments. To investigate the effect of hypoxia on uptake of exogenous Aβ, we treated all the SMC subtypes with fluorescently labeled Aβ40 and Aβ42 peptides. In compliance with an abundance of LRP1 expression found in cerebral vasculatures (Lillis et al., 2008), and the highest LRP1 expression showed in Figure 2C, NCSMCs demonstrated greatest uptake of Aβ40 and Aβ42 at 21% oxygen (Figure S2E). After the cells were cultured at 1% oxygen, hypoxia attenuated the amount of cell-associated Aβ, especially for NCSMCs (Aβ40, $p = 0.000324$; Aβ42, $p = 0.000723$) and NESMCs (Aβ40, $p = 0.000229$; Aβ42, $p = 0.000556$) (Figure 2D). On the other hand, the uptake of Aβ40 was not compromised in LMSMCs or PMSMCs under 1% oxygen, suggesting that such mesodermal derivatives may not mediate Aβ uptake primarily through LRP1-dependent pathway. Differences in Aβ metabolism among the SMC subtypes seemed to have already been influenced early by the differences in spatiotemporal development of neural crest and mesoderm. Nonneural crest SMC subtypes may not fully recapitulate the biology of cerebrovascular-specific attributes.

We further tested if in vitro Aβ metabolism could be assayed under more physiological conditions (Verghese et al., 2013). Uptake of Aβ in NCSMCs increased in a concentration-dependent manner (Figure S2F). We chose 300 ng/ml as a near-physiological concentration, which yielded a relatively well-detectable readout to proceed with Aβ uptake under 1% oxygen. Consistent with previous experiments, hypoxia attenuated the amount of cell-associated Aβ40 and Aβ42 in BVSMCs (Aβ40, $p = 0.00105$; Aβ42, $p = 0.00304$) and NCSMCs (Aβ40, $p = 0.00015$; Aβ42, $p = 0.00290$) (Figure S2G). However, no significant change was observed in NESMCs, suggesting that hypoxia-induced alteration to Aβ uptake at physiological range may not be reproducible in NESMCs. Hence, NCSMC was the most appropriate SMC subtype for reproducing the pathophysiological features of cerebral vasculatures in Aβ metabolism.

NCSMCs Recapitulate LRP1-Mediated Amyloid-β Clearance

SMC-specific knockout of *Lrp1* in an amyloid mouse model accelerated brain Aβ accumulation and CAA (Kanekiyo et al., 2012). LRP1 suppression in brain primary SMCs significantly diminished their ability to uptake and degrade exogenous Aβ. To study whether Aβ processing in NCSMCs was regulated by LRP1, we performed gene silencing of *LRP1* using small interfering RNA (siRNA). At least 3-fold reduction of LRP gene ($p = 0.0120$) (Figure S3A) and protein levels ($p = 0.00144$) (Figure 3A) was achieved in comparison to the scrambled siRNA controls. *LRP1* knockdown resulted in compromised uptake of both Aβ40 ($p = 0.0000558$) and Aβ42 ($p = 0.000101$) in NCSMCs (Figure 3B). Intracellular lysosomal degradation of Aβ following uptake also depends on the presence of LRP1 (Kanekiyo et al., 2012). To study Aβ clearance after cellular uptake, we employed the use of ELISAs. LRP1 siRNA- and scrambled siRNA-treated NCSMCs were first incubated with 5 μg/ml of human recombinant Aβ for 3 hr in serum-containing medium. Total cell lysates were then collected at days 0, 2, and 5 after uptake for analysis. NCSMCs had low endogenous Aβ before uptake (Figure 3C). After uptake, scrambled control NCSMCs possessed significantly higher amounts of Aβ40 ($p = 0.00103$) and Aβ42 ($p = 0.0224$) than the *LRP1* siRNA-treated NCSMCs. Intracellular Aβ decreased over time with LRP1 siRNA-treated NCSMCs showing slower rate of Aβ42 clearance than scrambled siRNA-treated NCSMCs (Figure 3D). By day 5, degradation of both Aβ40 ($p = 0.0495$) and Aβ42 ($p = 0.0432$) was significantly compromised by LRP1 silencing in NCSMCs. In the LRP1 siRNA-treated NCSMCs, we observed different rate of degradation with Aβ40 being cleared more efficiently than Aβ42. This could suggest that the presence of Aβ-degrading proteases could contribute to the differential degradation kinetics of distinct forms of Aβ (Leissring and Turner, 2013). Clearance of Aβ peptides was also affected in the positive control BVSMCs as evident in the significantly higher amounts of remnant Aβ40 ($p = 0.00336$) and Aβ42 ($p = 0.000291$) in the *LRP1* siRNA-treated BVSMCs after 2 days of degradation (Figure S3B). Other SMC subtypes appeared to have inconsistent extent of Aβ clearance in response to LRP1 silencing, indicating that SMCs of other embryonic origins might not fully recapitulate lipoprotein receptor-mediated Aβ metabolism.

To investigate whether LRP1 played a role in lysosomal degradation of Aβ in our NCSMCs, we used a lysotracker dye to image for any colocalization of fluorescently labeled Aβ with lysosomes. Live cells were monitored at days 0, 3, and 7 after 3 hr of Aβ uptake. The results supported the above finding that LRP1 siRNA-treated NCSMCs had compromised Aβ clearance as traces of incorporated Aβ in lysosomes were still found at days 3 and 7 but not for the control NCSMCs (Figure 3E). Like previously described in human cerebrovascular SMCs, we confirmed that LRP1 functioned in our NCSMCs to facilitate intracellular Aβ degradation. The involvement of other lipoprotein receptors and Aβ-degrading proteases in Aβ clearance can be further explored using our NCSMC system.

Amyloid pathology in the brain is often accompanied by SMC atrophy (Blaise et al., 2012). We also studied the effect of recombinant Aβ on cell death of NCSMCs. Hypoxic condition exacerbated apoptosis of NCSMCs as evident by annexin V staining (Figure S3C). Higher concentrations of recombinant Aβ only resulted in minor increase in the proportion of apoptotic cells at 1% oxygen. We recognized the limitation of modeling Aβ-induced SMC death in vitro as substantial SMC loss in the leptomeningeal artery of patients was a consequence of chronic exposure to Aβ deposits. Hence, for the aim of improving

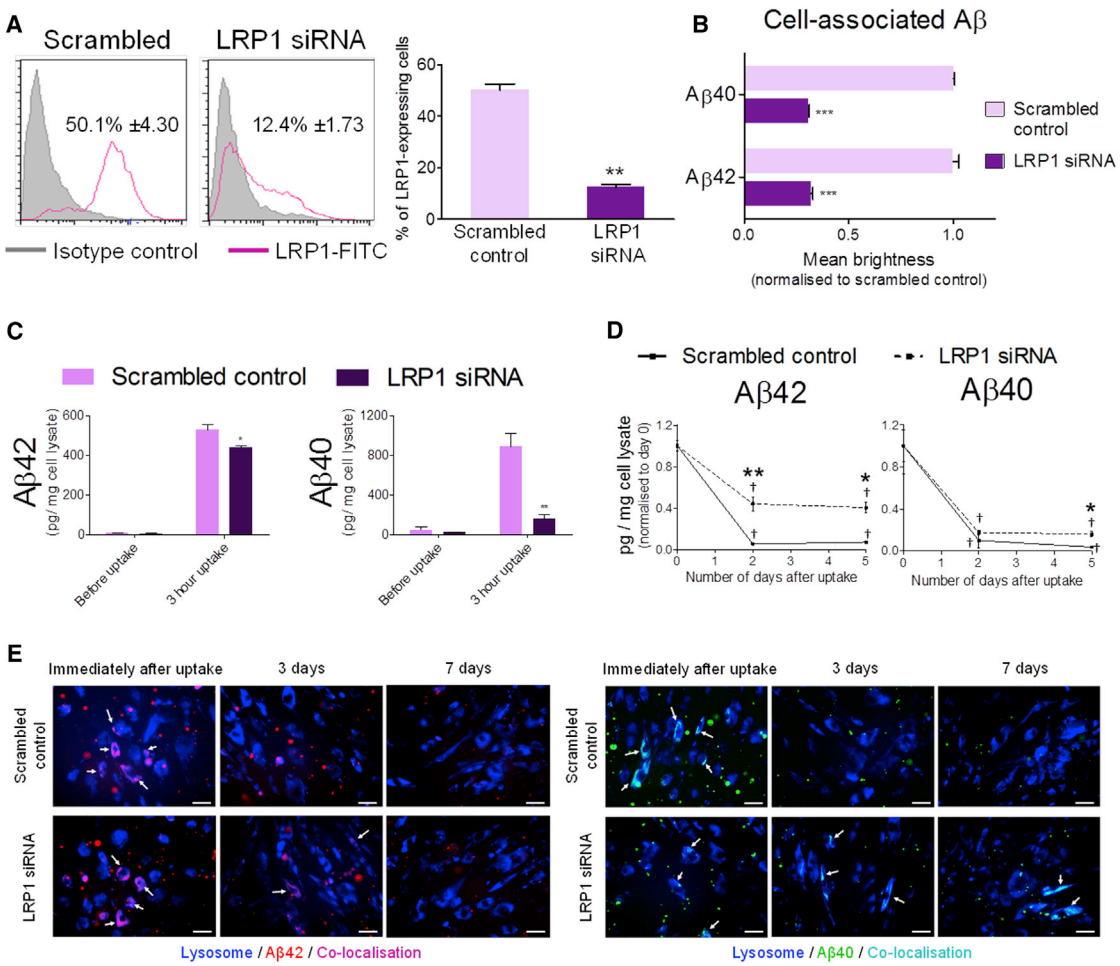

Figure 3. LRP1 Mediates Aβ Clearance in NCSMCs

(A) Flow cytometric analysis confirmed more than 3-fold LRP1 protein knockdown in *LRP1* siRNA-treated NCSMCs compared to scrambled control.

(B) LRP1 silencing in NCSMCs resulted in significantly reduced uptake of fluorescently labeled Aβ peptides in 3 hr as measured by flow cytometry.

(C) ELISA validated the decreased internalization of exogenous recombinant Aβ peptides in LRP1-suppressed NCSMCs after 3 hr uptake.

(D) Intracellular Aβ was monitored over time by ELISA on NCSMC cell lysates after 3 hr uptake of recombinant Aβ peptides. Aβ degradation was evident from the drop in Aβ levels by day 2, but NCSMCs with LRP1 knockdown were not as effective as scrambled controls in the elimination of internalized Aβ peptides.

(E) NCSMCs were imaged at days 0, 3, and 7 after a 3 hr uptake of fluorescently labeled Aβ40 (green) and Aβ42 (red) peptides. White arrows indicate incorporation of labeled Aβ in lysosomes (blue). Scale bar, 100 μm.

Data represent means ± SEM (n = 3). Statistical differences compared to scrambled controls were calculated with Student's t test for two groups or by ANOVA for three or more groups (*p < 0.05, **p < 0.01, **p < 0.001). See also Figure S3.

vascular health, NCSMCs could be used to develop a phenotypic assay of Aβ uptake.

High-Throughput Assay of Amyloid-β Uptake for Screening of Reference Compounds

To attain the eventual goal of cell-based phenotypic screening, we selected a panel of reference pharmaceutical compounds for testing. Patients on statin prescriptions for lowering circulating cholesterol to prevent cardiovascular diseases were reported to have lower incidence of neurodegenerative disorders and improved cognitive performance, probably due to pleiotropic vascular protective effects of drugs (Whitfield, 2007). Statins prevent late-onset Alzheimer's disease by stimulating LRP1 expression on brain vascular cells (Deane et al., 2004). Rifampicin, an antibiotic, enhances Aβ clearance by inducing LRP1 expression at the blood-brain barrier (Qosa et al., 2012). Another antibiotic, minocycline (Choi et al., 2007), and angiotensin receptor blockers (Li et al., 2010) are able to attenuate the progression of dementia, but there is not yet direct evidence that they target the Aβ clearance machinery. We tested the reference compounds on NCSMCs cultured at 1% oxygen and found that statins and rifampicin upregulated the gene and protein expressions of lipoprotein receptors (Figures 4A and 4B). These drugs were further evaluated for their potential benefits on Aβ uptake in NCSMCs.

To develop high-throughput screening capability on our NCSMCs, we had to choose a sensitive and disease-relevant readout, in this case, uptake of labeled Aβ peptides. We scaled

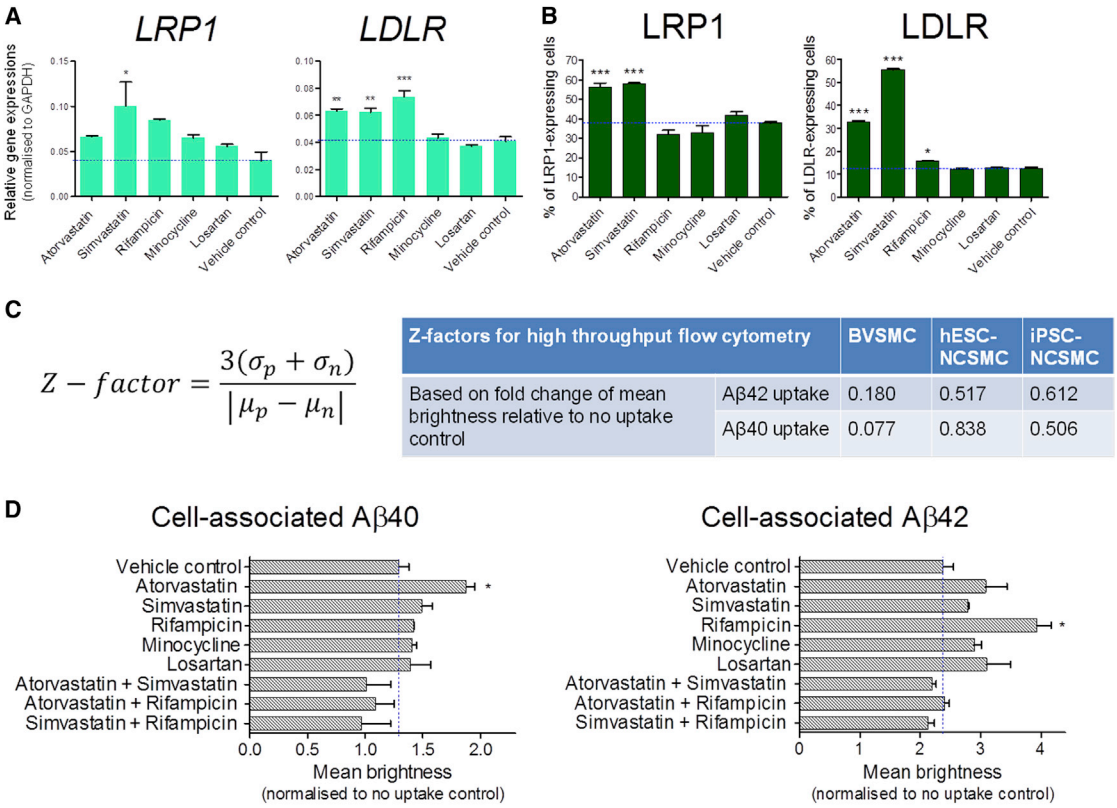

Z-factors for high throughput flow cytometry		BVSMC	hESC-NCSMC	iPSC-NCSMC
Based on fold change of mean brightness relative to no uptake control	Aβ42 uptake	0.180	0.517	0.612
	Aβ40 uptake	0.077	0.838	0.506

Figure 4. Testing of Vascular Protective Compounds in a High-Throughput Aβ Uptake Assay

(A) Reference drugs were treated on NCSMCs at 1% oxygen for 48 hr to investigate whether the compounds could rescue the compromised gene expressions of lipoprotein receptors by chronic hypoxia.

(B) Flow cytometric analysis of LRP1 and LDLR protein expression after 48 hr of compound treatment on NCSMCs at 1% oxygen.

(C) Z factor is a statistical measurement of the feasibility of a cell-based phenotypic assay for high-throughput screening. Average measurements on "fold change of mean brightness relative to no-uptake control" and SDs were obtained from positive (grown at 21% oxygen) and negative (grown at 1% oxygen) controls. The means and SDs of both positive (p) and negative (n) controls are indicated as (μ_p, σ_p) and (μ_n, σ_n), respectively. A value of more than 0.5 indicates a robust Aβ uptake assay, whereas a value of between 0 and 0.5 is a marginal assay.

(D) Reference drugs were treated on NCSMCs for 48 hr prior to uptake of fluorescently labeled Aβ peptides for an hour in a 96-well plate format. Cell-associated Aβ was evaluated by high-throughput flow cytometry.

Data represent means ± SEM (n = 3). Statistical differences compared to vehicle controls were calculated with Student's t test (*p < 0.05, **p < 0.01, **p < 0.001). See also Figure S3.

down the NCSMC and BVSMC cultures to 96-well format. A plating density of 30,000 cells/well yielded good postthawing survival and reproducibility for assessment of Aβ uptake. SMCs, which were routinely grown at 21% oxygen, represented the positive control, whereas SMCs conditioned to chronic hypoxia at 1% oxygen were used as the negative control and experimental samples. Cells were incubated with labeled Aβ40 and Aβ42 (2 μg/ml) for an hour and subsequently evaluated by high-throughput flow cytometry. Aβ uptake in NCSMCs derived from both hESC (H9) and iPSC (KYOUDXR0109B) resulted in Z-factors of more than 0.5, indicative of a statistically robust assay (Figure 4C). On the other hand, BVSMC produced a Z-factor between 0 and 0.5, which was considered only a marginal assay. To prove the feasibility of drug screening, NCSMCs derived from hESC (H9) were treated with reference compounds and vehicle control for 48 hr, followed by uptake of Aβ for another hour. Among these reference compounds, only statins and rifampicin were reported to exert direct effects on upregulating LRP1 and LDLR expression (Qosa et al., 2012; Pocathikorn et al., 2010; Deane et al., 2004). Our findings revealed that atorvastatin (p = 0.0492) and rifampicin (p = 0.0174) significantly increased Aβ40 and Aβ42 uptake, respectively, in NCSMCs over the vehicle controls (Figure 4D). This could be due to increased expression of the lipoprotein receptors although the effects of such compounds on Aβ uptake may occur through other mechanisms as well. Minocycline and losartan may not have any apparent effect and could be further investigated by a dose-response experiment. Drug combinations appeared to be countereffective because there were no significant beneficial effects over the control. Likewise, NCSMCs derived from human iPSC (KYOUDXR0109B) had identified rifampicin, which could improve Aβ uptake (Figure S3D), supporting the robustness of NCSMC model for phenotypic screening. Taken together, we have established a cell-based platform that is amenable for

high-throughput screening of novel compounds and for unraveling beneficial effects of vascular protective compounds.

DISCUSSION

Vascular SMCs exist in a wide range of anatomic locations. Gene expression profiling of SMCs from various tissues revealed heterogeneity in molecular signatures (Chi et al., 2007). The use of appropriate SMC subtypes will be imperative for modeling the functional and organ specializations (Majesky and Mummery, 2012). Capitalizing on the fact that cerebral SMCs could contribute to Aβ elimination by intracellular degradation, we have derived NCSMCs of a neural crest origin in order to reproduce characteristics of neurovascular Aβ metabolism. Indeed, NCSMCs demonstrated more profound deficits in Aβ uptake than the other lineage-specific SMCs upon chronic hypoxic treatment. Such intrinsic differences among SMC subtypes could be attributed to their diverse embryonic origins. Success of a cell-based assay will therefore rely on suitable lineage-derived cell type, which is able to yield disease-relevant phenotypic readouts. We also recognize that other Aβ clearance pathways could be better modeled in the presence of additional cell types such as endothelial cells and astrocytes. There have been progresses in obtaining brain-specific endothelial cells (Lippmann et al., 2012) and astrocytes (Krencik and Zhang, 2011) from hPSCs. This will open up avenues to create organotypic system of the neurovascular unit toward the understanding of CAA pathogenesis and neurological disorders.

CAA can be a multifactorial outcome due to environmental and genetic predispositions. Besides hypoxia, Aβ-induced NADPH oxidase activation plays a part in vascular oxidative stress, leading to cerebrovascular dysfunction (Park et al., 2005). Arterial stiffening in the aging brain diminishes the pulsatile forces for drainage of interstitial fluid and solutes, causing Aβ deposits in the perivascular regions as CAA (Weller et al., 2009). Elevated levels of inflammatory cytokines are also evident in the brain microvasculature of Alzheimer's disease individuals (Gorelick et al., 2011). Our NCSMC resource can be adapted to interrogate the effects of such risk factors. Genetic susceptibility to CAA has been commonly studied in transgenic mice with mutant forms of APP, which influence abnormal Aβ metabolism and aggregation (Herzig et al., 2004; Winkler et al., 2001). Patients with hereditary cerebral amyloidosis were found to develop severe CAA, along with hemorrhagic strokes and vascular dementia due to SMC degeneration (Fossati et al., 2010). On the other hand, the differences in apolipoprotein E (APOE) genotypes seem to have notable effect on the course of sporadic CAA as SMCs can internalize Aβ via the lipoprotein pathway involving APOE (Ruzali et al., 2013). Carrier of APOE4 showed increased incidence of Aβ accumulation, rendering the vessel walls more prone to vasculopathic rupture (Strittmatter et al., 1993; Schmechel et al., 1993; Mazur-Kolecka et al., 2003). Patient iPSCs will provide a valuable channel to capture these complex genotypes that predispose them to CAA. Patient NCSMCs generated from such diseased iPSCs will serve as a useful model to study CAA-associated pathological changes.

HPSC-based phenotypic screening is gaining momentum as a potential preclinical strategy for drug discovery (Zhang et al., 2014; Lee et al., 2012; Höing et al., 2012; Yang et al., 2013). As compared to the conventional hypothesis-driven target-based screening, the phenotypic approach seeks to identify candidate compounds with desired effects, without knowing the molecular mechanism of action of drugs. Albeit more difficult to subsequently design chemical modifications for better results, phenotypic assay will be highly complementary as a secondary screening to validate primary hits. In this work, our pilot testing of pharmaceutical compounds is proof of concept that vascular protective agents could mediate Aβ uptake by SMCs in a high-throughput manner. Many of these marketed compounds have activity against vascular targets and have proven safety in patients (Guan et al., 2011). Our NCSMC platform can also be used in screening a smaller panel of FDA-approved drugs for ameliorating vascular complications in neurological indications. Drug repurposing by cell-based phenotypic assay can identify previously unknown therapeutic effects in order to inform further mechanistic analysis, thereby shortening the lead time to clinic.

EXPERIMENTAL PROCEDURES

Detailed experimental and analysis methods can be found in the Supplemental Experimental Procedures.

HPSC Maintenance

H9 HESC line (WiCell) was cultured in a chemically defined medium (CDM) as previously described (Brons et al., 2007). Human iPSCs were obtained by reprogramming human foreskin fibroblasts (BJs) into transgene-free iPSCs by the Sendai viral vector method. These BJ-iPSCs were grown on irradiated mouse feeders and cultured in DMEM/F12 medium, containing 20% Knockout serum replacement (Gibco) and 4 ng/ml FGF-2 (R&D Systems). We have also used commercially available human iPSCs (KYOUDXR0109B, ATCC), which were derived from dermal fibroblasts obtained from a healthy adult donor. These fibroblasts were reprogrammed by the expression of *OCT4*, *SOX2*, *KLF4*, and *MYC* using retroviral transduction and subsequently cultured in the conditions as stated above.

NCSMC Differentiation

For neural crest differentiation, hPSCs were grown in CDM + bFGF (12 ng/ml, R&D systems) + SB431542 (10 μM, Sigma) + noggin (200 ng/ml, R&D Systems) for 10–13 days, with change of medium every 2–3 days. After which, $NGFR^+$/$B3GAT1^+$ cells were isolated by fluorescence-activated cell sorting (FACS) and replated for SMC induction. Sorted cells were cultured in SMC differentiation medium CDM + PDGF-BB (10 ng/ml, PeproTech) + TGF-β1 (2 ng/ml, PeproTech) for another 12 days. Derived NCSMCs could be propagated further in culture using SMC medium (SC-1101, Sciencell). All experiments were done on NCSMCs between passages 1 and 9. On the other hand, the other SMC subtypes (NESMC, LMSMC, and PMSMC) were generated by a previously established protocol (Cheung et al., 2012).

Source of BVSMCs

The human brain vascular smooth muscle cells (BVSMCs) were acquired from a commercial source, ScienCell Research Laboratories (cat no. #1100) and cultured using SMC medium (SC-1101, Sciencell). All experiments were done on BVSMCs between passages 1 and 9. The SMC medium contains essential and nonessential amino acids, vitamins, organic and inorganic compounds, hormones, growth factors, trace minerals and fetal bovine serum, smooth muscle growth supplements, and penicillin/streptomycin solution.

Aβ Peptide Uptake Measurement by Flow Cytometry

SMC subtypes were incubated with 2 μg/ml of fluorescently labeled amyloid peptide (Aβ42-Hilyte Fluor 555 or Aβ40-Hilyte Fluor 488, Anaspec) at 37°C

for a 3 hr uptake unless otherwise stated. After Aβ uptake, cells were dissociated into single-cell suspension for flow cytometric analysis by Becton Dickinson FACSCalibur. Mean fluorescence brightness was calculated from each Aβ uptake sample in triplicates and normalized to the mean fluorescence brightness of no-uptake control samples. Relative comparisons of cell-associated Aβ in SMC subtypes were then plotted.

High-Throughput Aβ Uptake Assay Development

NCSMCs and BVSMCs were routinely cultured at 21% oxygen and 1% oxygen to simulate normoxic and chronic hypoxic conditions, respectively. Twenty-one percent O_2 SMCs were seeded at 30,000 cells/well onto 96-well plate as positive controls. One percent O_2 SMCs were seeded at the same density as negative controls and experimental samples for drug treatment on the same plate. The 96-well plate was incubated at 37°C overnight at 21% O_2. After cell attachment, 2 μg/ml of fluorescently labeled amyloid peptide (Aβ42-Hilyte Fluor 555 or Aβ40-Hilyte Fluor 488, Anaspec) was added to SMCs for a 1 hr uptake at 37°C. After Aβ uptake, cells were dissociated into single-cell suspension for high-throughput flow cytometry by LSRFortessa plate analyzer. Respective Z factors for NCSMC and BVSMC Aβ uptake assays were calculated based on their mean fluorescence brightness (normalized to no-uptake controls) and SDs of positive (21% O_2) and negative (1% O_2) controls. For the experimental samples with drug treatment, NCSMCs were incubated with reference compounds (i.e., atorvastatin, simvastatin, rifampicin, minocycline, losartan, and vehicle control) for 48 hr prior to Aβ uptake. Mean fluorescence brightness signals (normalized to no-uptake control) indicated the degree of amyloid uptake.

Statistical Analysis

Results are presented as mean ± SEM of three independent experiments unless otherwise stated. Statistical p values were calculated by Student's t test for two groups or by ANOVA for three or more groups. Significant differences are indicated as *$p < 0.05$, **$p < 0.01$, and **$p < 0.001$ unless otherwise stated.

ACCESSION NUMBERS

The Gene Expression accession number for microarray data reported in this paper is GSE55173.

SUPPLEMENTAL INFORMATION

Supplemental Information includes Supplemental Experimental Procedures, three figures, one table, and four movies and can be found with this article online at http://dx.doi.org/10.1016/j.celrep.2014.08.065.

AUTHOR CONTRIBUTIONS

C.C. supervised and conceived the idea for this work, performed experiments, analyzed data, and wrote the paper. Y.T.G. and C.W. performed experiments and analyzed data. J.Z. and E.G. contributed to microarray data analysis and manuscript editing.

ACKNOWLEDGMENTS

We are grateful to Dr. Lee May Ann for advice on cell-based assay development, Prof. Jean Paul Thiery's lab for offering us their hypoxic chamber, Dr. Sanjay Sinha for data discussion, Dr. Jonathan Loh for providing us with BJ-iPSCs, and Molecular Engineering Laboratory (Singapore) for the HeLa cells and neuronal antibodies. This research was funded by the Independent Fellowship from the Institute of Molecular and Cell Biology, Singapore.

Received: February 19, 2014
Revised: June 30, 2014
Accepted: August 25, 2014
Published: October 2, 2014

REFERENCES

Alonzo, N.C., Hyman, B.T., Rebeck, G.W., and Greenberg, S.M. (1998). Progression of cerebral amyloid angiopathy: accumulation of amyloid-beta40 in affected vessels. J. Neuropathol. Exp. Neurol. *57*, 353–359.

Bell, R.D., Deane, R., Chow, N., Long, X., Sagare, A., Singh, I., Streb, J.W., Guo, H., Rubio, A., Van Nostrand, W., et al. (2009). SRF and myocardin regulate LRP-mediated amyloid-beta clearance in brain vascular cells. Nat. Cell Biol. *11*, 143–153.

Blaise, R., Mateo, V., Rouxel, C., Zaccarini, F., Glorian, M., Béréziat, G., Golubkov, V.S., and Limon, I. (2012). Wild-type amyloid beta 1-40 peptide induces vascular smooth muscle cell death independently from matrix metalloprotease activity. Aging Cell *11*, 384–393.

Brons, I.G., Smithers, L.E., Trotter, M.W., Rugg-Gunn, P., Sun, B., Chuva de Sousa Lopes, S.M., Howlett, S.K., Clarkson, A., Ahrlund-Richter, L., Pedersen, R.A., and Vallier, L. (2007). Derivation of pluripotent epiblast stem cells from mammalian embryos. Nature *448*, 191–195.

Calhoun, M.E., Burgermeister, P., Phinney, A.L., Stalder, M., Tolnay, M., Wiederhold, K.H., Abramowski, D., Sturchler-Pierrat, C., Sommer, B., Staufenbiel, M., and Jucker, M. (1999). Neuronal overexpression of mutant amyloid precursor protein results in prominent deposition of cerebrovascular amyloid. Proc. Natl. Acad. Sci. USA *96*, 14088–14093.

Chambers, S.M., Fasano, C.A., Papapetrou, E.P., Tomishima, M., Sadelain, M., and Studer, L. (2009). Highly efficient neural conversion of human ES and iPS cells by dual inhibition of SMAD signaling. Nat. Biotechnol. *27*, 275–280.

Cheung, C., and Sinha, S. (2011). Human embryonic stem cell-derived vascular smooth muscle cells in therapeutic neovascularisation. J. Mol. Cell. Cardiol. *51*, 651–664.

Cheung, C., Bernardo, A.S., Trotter, M.W., Pedersen, R.A., and Sinha, S. (2012). Generation of human vascular smooth muscle subtypes provides insight into embryological origin-dependent disease susceptibility. Nat. Biotechnol. *30*, 165–173.

Chi, J.T., Rodriguez, E.H., Wang, Z., Nuyten, D.S., Mukherjee, S., van de Rijn, M., van de Vijver, M.J., Hastie, T., and Brown, P.O. (2007). Gene expression programs of human smooth muscle cells: tissue-specific differentiation and prognostic significance in breast cancers. PLoS Genet. *3*, 1770–1784.

Choi, Y., Kim, H.S., Shin, K.Y., Kim, E.M., Kim, M., Kim, H.S., Park, C.H., Jeong, Y.H., Yoo, J., Lee, J.P., et al. (2007). Minocycline attenuates neuronal cell death and improves cognitive impairment in Alzheimer's disease models. Neuropsychopharmacology *32*, 2393–2404.

Deane, R., and Zlokovic, B.V. (2007). Role of the blood-brain barrier in the pathogenesis of Alzheimer's disease. Curr. Alzheimer Res. *4*, 191–197.

Deane, R., Wu, Z., and Zlokovic, B.V. (2004). RAGE (yin) versus LRP (yang) balance regulates alzheimer amyloid beta-peptide clearance through transport across the blood-brain barrier. Stroke *35* (11, Suppl 1), 2628–2631.

Farkas, E., and Luiten, P.G. (2001). Cerebral microvascular pathology in aging and Alzheimer's disease. Prog. Neurobiol. *64*, 575–611.

Fossati, S., Cam, J., Meyerson, J., Mezhericher, E., Romero, I.A., Couraud, P.O., Weksler, B.B., Ghiso, J., and Rostagno, A. (2010). Differential activation of mitochondrial apoptotic pathways by vasculotropic amyloid-beta variants in cells composing the cerebral vessel walls. FASEB J. *24*, 229–241.

Gorelick, P.B., Scuteri, A., Black, S.E., Decarli, C., Greenberg, S.M., Iadecola, C., Launer, L.J., Laurent, S., Lopez, O.L., Nyenhuis, D., et al.; American Heart Association Stroke Council, Council on Epidemiology and Prevention, Council on Cardiovascular Nursing, Council on Cardiovascular Radiology and Intervention, and Council on Cardiovascular Surgery and Anesthesia (2011). Vascular contributions to cognitive impairment and dementia: a statement for healthcare professionals from the american heart association/american stroke association. Stroke *42*, 2672–2713.

Guan, W., Kozak, A., and Fagan, S.C. (2011). Drug repurposing for vascular protection after acute ischemic stroke. Acta Neurochir. Suppl. (Wien) *111*, 295–298.

Herzig, M.C., Winkler, D.T., Burgermeister, P., Pfeifer, M., Kohler, E., Schmidt, S.D., Danner, S., Abramowski, D., Stürchler-Pierrat, C., Bürki, K., et al. (2004). Abeta is targeted to the vasculature in a mouse model of hereditary cerebral hemorrhage with amyloidosis. Nat. Neurosci. *7*, 954–960.

Höing, S., Rudhard, Y., Reinhardt, P., Glatza, M., Stehling, M., Wu, G., Peiker, C., Böcker, A., Parga, J.A., Bunk, E., et al. (2012). Discovery of inhibitors of microglial neurotoxicity acting through multiple mechanisms using a stem-cell-based phenotypic assay. Cell Stem Cell *11*, 620–632.

Hu, B.Y., and Zhang, S.C. (2009). Differentiation of spinal motor neurons from pluripotent human stem cells. Nat. Protoc. *4*, 1295–1304.

Jellinger, K.A. (2010). Prevalence and impact of cerebrovascular lesions in Alzheimer and lewy body diseases. Neurodegener. Dis. *7*, 112–115.

Kanekiyo, T., Liu, C.C., Shinohara, M., Li, J., and Bu, G. (2012). LRP1 in brain vascular smooth muscle cells mediates local clearance of Alzheimer's amyloid-β. J. Neurosci. *32*, 16458–16465.

Krencik, R., and Zhang, S.C. (2011). Directed differentiation of functional astroglial subtypes from human pluripotent stem cells. Nat. Protoc. *6*, 1710–1717.

Lee, G., Ramirez, C.N., Kim, H., Zeltner, N., Liu, B., Radu, C., Bhinder, B., Kim, Y.J., Choi, I.Y., Mukherjee-Clavin, B., et al. (2012). Large-scale screening using familial dysautonomia induced pluripotent stem cells identifies compounds that rescue IKBKAP expression. Nat. Biotechnol. *30*, 1244–1248.

Lefterov, I., Fitz, N.F., Cronican, A.A., Fogg, A., Lefterov, P., Kodali, R., Wetzel, R., and Koldamova, R. (2010). Apolipoprotein A-I deficiency increases cerebral amyloid angiopathy and cognitive deficits in APP/PS1DeltaE9 mice. J. Biol. Chem. *285*, 36945–36957.

Leissring, M.A., and Turner, A.J. (2013). Regulation of distinct pools of amyloid β-protein by multiple cellular proteases. Alzheimers Res. Ther. *5*, 37.

Li, N.C., Lee, A., Whitmer, R.A., Kivipelto, M., Lawler, E., Kazis, L.E., and Wolozin, B. (2010). Use of angiotensin receptor blockers and risk of dementia in a predominantly male population: prospective cohort analysis. BMJ *340*, b5465.

Li, W., Xiong, Y., Shang, C., Twu, K.Y., Hang, C.T., Yang, J., Han, P., Lin, C.Y., Lin, C.J., Tsai, F.C., et al. (2013). Brg1 governs distinct pathways to direct multiple aspects of mammalian neural crest cell development. Proc. Natl. Acad. Sci. USA *110*, 1738–1743.

Lillis, A.P., Van Duyn, L.B., Murphy-Ullrich, J.E., and Strickland, D.K. (2008). LDL receptor-related protein 1: unique tissue-specific functions revealed by selective gene knockout studies. Physiol. Rev. *88*, 887–918.

Lippmann, E.S., Azarin, S.M., Kay, J.E., Nessler, R.A., Wilson, H.K., Al-Ahmad, A., Palecek, S.P., and Shusta, E.V. (2012). Derivation of blood-brain barrier endothelial cells from human pluripotent stem cells. Nat. Biotechnol. *30*, 783–791.

Majesky, M.W. (2007). Developmental basis of vascular smooth muscle diversity. Arterioscler. Thromb. Vasc. Biol. *27*, 1248–1258.

Majesky, M.W., and Mummery, C.L. (2012). Smooth muscle diversity from human pluripotent cells. Nat. Biotechnol. *30*, 152–154.

Mazur-Kolecka, B., Kowal, D., Sukontasup, T., Dickson, D., and Frackowiak, J. (2003). The effect of oxidative stress on accumulation of apolipoprotein E3 and E4 in a cell culture model of beta-amyloid angiopathy (CAA). Brain Res. *983*, 48–57.

Menendez, L., Kulik, M.J., Page, A.T., Park, S.S., Lauderdale, J.D., Cunningham, M.L., and Dalton, S. (2013). Directed differentiation of human pluripotent cells to neural crest stem cells. Nat. Protoc. *8*, 203–212.

Miners, J.S., Van Helmond, Z., Chalmers, K., Wilcock, G., Love, S., and Kehoe, P.G. (2006). Decreased expression and activity of neprilysin in Alzheimer disease are associated with cerebral amyloid angiopathy. J. Neuropathol. Exp. Neurol. *65*, 1012–1021.

Nedergaard, M. (2013). Neuroscience. Garbage truck of the brain. Science *340*, 1529–1530.

Park, L., Anrather, J., Zhou, P., Frys, K., Pitstick, R., Younkin, S., Carlson, G.A., and Iadecola, C. (2005). NADPH-oxidase-derived reactive oxygen species mediate the cerebrovascular dysfunction induced by the amyloid beta peptide. J. Neurosci. *25*, 1769–1777.

Pocathikorn, A., Taylor, R.R., and Mamotte, C.D. (2010). Atorvastatin increases expression of low-density lipoprotein receptor mRNA in human circulating mononuclear cells. Clin. Exp. Pharmacol. Physiol. *37*, 471–476.

Qosa, H., Abuznait, A.H., Hill, R.A., and Kaddoumi, A. (2012). Enhanced brain amyloid-β clearance by rifampicin and caffeine as a possible protective mechanism against Alzheimer's disease. J. Alzheimers Dis. *31*, 151–165.

Rovelet-Lecrux, A., Hannequin, D., Raux, G., Le Meur, N., Laquerrière, A., Vital, A., Dumanchin, C., Feuillette, S., Brice, A., Vercelletto, M., et al. (2006). APP locus duplication causes autosomal dominant early-onset Alzheimer disease with cerebral amyloid angiopathy. Nat. Genet. *38*, 24–26.

Ruzali, W.A., Kehoe, P.G., and Love, S. (2013). Influence of LRP-1 and apolipoprotein E on amyloid-β uptake and toxicity to cerebrovascular smooth muscle cells. J. Alzheimers Dis. *33*, 95–110.

Schmechel, D.E., Saunders, A.M., Strittmatter, W.J., Crain, B.J., Hulette, C.M., Joo, S.H., Pericak-Vance, M.A., Goldgaber, D., and Roses, A.D. (1993). Increased amyloid beta-peptide deposition in cerebral cortex as a consequence of apolipoprotein E genotype in late-onset Alzheimer disease. Proc. Natl. Acad. Sci. USA *90*, 9649–9653.

Shi, X., Fu, Y., Liao, D., Chen, Y., and Liu, J. (2014). Alterations of voltage-dependent calcium channel currents in basilar artery smooth muscle cells at early stage of subarachnoid hemorrhage in a rabbit model. PLoS ONE *9*, e84129.

Sleegers, K., Brouwers, N., Gijselinck, I., Theuns, J., Goossens, D., Wauters, J., Del-Favero, J., Cruts, M., van Duijn, C.M., and Van Broeckhoven, C. (2006). APP duplication is sufficient to cause early onset Alzheimer's dementia with cerebral amyloid angiopathy. Brain *129*, 2977–2983.

Soffer, D. (2006). Cerebral amyloid angiopathy—a disease or age-related condition. Isr. Med. Assoc. J. *8*, 803–806.

Strittmatter, W.J., Saunders, A.M., Schmechel, D., Pericak-Vance, M., Enghild, J., Salvesen, G.S., and Roses, A.D. (1993). Apolipoprotein E: high-avidity binding to beta-amyloid and increased frequency of type 4 allele in late-onset familial Alzheimer disease. Proc. Natl. Acad. Sci. USA *90*, 1977–1981.

Urmoneit, B., Prikulis, I., Wihl, G., D'Urso, D., Frank, R., Heeren, J., Beisiegel, U., and Prior, R. (1997). Cerebrovascular smooth muscle cells internalize Alzheimer amyloid beta protein via a lipoprotein pathway: implications for cerebral amyloid angiopathy. Lab. Invest. *77*, 157–166.

Verghese, P.B., Castellano, J.M., Garai, K., Wang, Y., Jiang, H., Shah, A., Bu, G., Frieden, C., and Holtzman, D.M. (2013). ApoE influences amyloid-β (Aβ) clearance despite minimal apoE/Aβ association in physiological conditions. Proc. Natl. Acad. Sci. USA *110*, E1807–E1816.

Viswanathan, A., and Greenberg, S.M. (2011). Cerebral amyloid angiopathy in the elderly. Ann. Neurol. *70*, 871–880.

Wang, Z., Yang, D., Zhang, X., Li, T., Li, J., Tang, Y., and Le, W. (2011). Hypoxia-induced down-regulation of neprilysin by histone modification in mouse primary cortical and hippocampal neurons. PLoS ONE *6*, e19229.

Wang, A., Tang, Z., Li, X., Jiang, Y., Tsou, D.A., and Li, S. (2012). Derivation of smooth muscle cells with neural crest origin from human induced pluripotent stem cells. Cells Tissues Organs (Print) *195*, 5–14.

Weller, R.O., Preston, S.D., Subash, M., and Carare, R.O. (2009). Cerebral amyloid angiopathy in the aetiology and immunotherapy of Alzheimer disease. Alzheimers Res. Ther. *1*, 6.

Whitfield, J.F. (2007). The road to LOAD: late-onset Alzheimer's disease and a possible way to block it. Expert Opin. Ther. Targets *11*, 1257–1260.

Wilhelmus, M.M., Otte-Höller, I., van Triel, J.J., Veerhuis, R., Maat-Schieman, M.L., Bu, G., de Waal, R.M., and Verbeek, M.M. (2007). Lipoprotein receptor-related protein-1 mediates amyloid-beta-mediated cell death of cerebrovascular cells. Am. J. Pathol. *171*, 1989–1999.

Winkler, D.T., Bondolfi, L., Herzig, M.C., Jann, L., Calhoun, M.E., Wiederhold, K.H., Tolnay, M., Staufenbiel, M., and Jucker, M. (2001). Spontaneous

hemorrhagic stroke in a mouse model of cerebral amyloid angiopathy. J. Neurosci. *21*, 1619–1627.

Yang, Y.M., Gupta, S.K., Kim, K.J., Powers, B.E., Cerqueira, A., Wainger, B.J., Ngo, H.D., Rosowski, K.A., Schein, P.A., Ackeifi, C.A., et al. (2013). A small molecule screen in stem-cell-derived motor neurons identifies a kinase inhibitor as a candidate therapeutic for ALS. Cell Stem Cell *12*, 713–726.

Yao, Y., Chen, Z.L., Norris, E.H., and Strickland, S. (2014). Astrocytic laminin regulates pericyte differentiation and maintains blood brain barrier integrity. Nat. Commun. *5*, 3413.

Zhang, M., Luo, G., Zhou, Y., Wang, S., and Zhong, Z. (2014). Phenotypic screens targeting neurodegenerative diseases. J. Biomol. Screen. *19*, 1–16.

Zlokovic, B.V. (2011). Neurovascular pathways to neurodegeneration in Alzheimer's disease and other disorders. Nat. Rev. Neurosci. *12*, 723–738.

Zuloaga, K.L., and Gonzales, R.J. (2011). Dihydrotestosterone attenuates hypoxia inducible factor-1α and cyclooxygenase-2 in cerebral arteries during hypoxia or hypoxia with glucose deprivation. Am. J. Physiol. Heart Circ. Physiol. *301*, H1882–H1890.